DOI: 10.6060/mhc256515L

Electropolymerized Metallocorroles (M = Co, Cu, Mn) for Enhanced Electrocatalyzed Oxygen Reductions

Yu Chen,[a] Minyu Jiang,[b] Shibin Zhu,[a] Yunlong Pan,[b] Jing Xu,[a@1] and Xu Liang[b@2]

[a]*School of Physics and Electronic Engineering, Jiangsu University, Zhenjiang 212013, P. R. China*
[b]*School of Chemistry and Chemical Engineering, Jiangsu University, Zhenjiang 212013, P. R. China*
[@1]*Corresponding author E-mail: xjing@ujs.edu.cn*
[@2]*Corresponding author E-mail: liangxu@ujs.edu.cn*

*Herein, a series of three M^{III}corrole monomers were used and their related polymers were prepared through facile and environmentally friendly electropolymerization methods. Upon functionalized on the electrodes, these metallocorrole based polymers exhibited the enhanced and tunable electrochemically catalyzed oxygen reduction reactions. Especially, the electron transfer numbers (n) of the oxidation-reaction process of three polymers **p-1a-c** were n = 3.67, 3.43, and 3.63 which tended to be converted to water through selective four electrons ($4e^-$) oxygen reductions.*

Keywords: Metallocorroles, electropolymerization, oxygen reductions, electrocatalysis, functionalized electrodes.

Электрополимеризованные металлокорролы (M = Co, Cu, Mn) для улучшенного электрокаталитического восстановления кислорода

Юй Чэнь,[a] Миньюй Цзян,[b] Шибинь Чжу,[a] Юньлун Пань,[b] Цзин Сюй,[a@1] Сюй Лян[b@2]

[a]*Факультет физики и электронной инженерии, Университет Цзянсу, Чжэньцзян 212013, Китайская Народная Республика*
[b]*Факультет химии и химической инженерии, Университет Цзянсу, Чжэньцзян 212013, Китайская Народная Республика*
[@1]*E-mail: xjing@ujs.edu.cn*
[@2]*E-mail: liangxu@ujs.edu.cn*

*В данной работе была использована серия из трёх мономеров металлокорролов и их полимеров на их основе, полученных простыми и экологически безопасными методами электрополимеризации. После функционализации на электродах этих полимеров числа переноса электронов (n) в процессе реакции электрохимического восстановления кислорода, катализируемых тремя полимерами **p-1a-c**, составили n = 3,67, 3,43 и 3,63, что свидетельствует о наличии тенденции к превращению в воду посредством селективного четырёхэлектронного восстановления кислорода (4e-).*

Ключевые слова: Металлокорролы, электрополимеризация, восстановление кислорода, электрокатализ, функционализированные электроды.

Introduction

In 1977, Hideki Shirakawa's group discovered the conductivity of doped polyacetylene, a breakthrough that completely rewrote the history of insulating materials science, for which they were awarded the Nobel Prize in Chemistry in 2000.[1-3] The conductivity mystery of organic conductive polymers lies in their unique conjugated structure, which, by alternating arrangement of single and double bond systems, forms delocalized π-electron clouds, that create high-speed conductive channels on the molecular chain.[4-6] For example, materials with adjustable conductivity properties such as polypyrrole and polyaniline were elaborated.[7-8] Especially the conductivity of polyaniline/graphene composite material has exceeded 5000 S/cm, comparable to the conductivity of metallic silver.[9] Importantly, the organic conductive polymers have widely applied in the field of flexible electronics.[10-12] For example, the foldable OLED screen uses poly (3,4-ethylenedioxythiophene) as the transparent electrode, with a light transmittance of over 90% and a bending resistance of over 100000 times.[13] In addition, the organic conductive polymers are well applied for biomedicine like polypyrrole sensors, that can detect biomolecules at a concentration of 0.1 nM in real time, providing a new tool for precision medicine.[14-15] On the other hand, the field of new energy is witnessing a revolutionary breakthrough in organic conductive polymers.[16-17] The conversion efficiency of organic solar cells constructed from polythiophene derivatives has reached 18.7%, while supercapacitors based on polyaniline can be charged within 3 s with a cycle life of over 100000 times.[18-19] With the advancement of molecular engineering and nanotechnology, organic conductive polymers are breaking through the bottleneck of conductivity and stability.[20] Scientists predict that within the next decade, such materials will bring disruptive innovations in fields such as neural electrodes, smart skin, and space cables, redefining the boundaries of human understanding of "conductivity".

On the other hand, metallocorroles are a type of functional molecule formed by chelation of tetrapyrrole macrocyclic clathrate ligands with metal ions.[21-22] Their unique molecular and electronic structure are becoming star molecules in the field of coordination chemistry and material science.[23] Compared with regular tetraphenylporphyrins,[24] the ring-contracted structure and the direct connected "C-C" bond results the stronger coordination ability and redox activity, providing a new paradigm for designing high-performance catalysts and functional materials.[25-27] In order to programmably control the molecular and electronic structures, a series of methods could be applied. Upon selecting the suitable central-ions (such as iron, cobalt, copper) and regulating the *meso*-/β-/axial-substituents, scientists can precisely modulate the photoelectric properties and catalytic activities.[28-30] For example, Co^{III}corroles exhibit competitive performance to platinum catalysts in oxygen reduction reactions with overpotentials as low as 320 mV, opening up a new path for fuel cell cathode materials.[31] Also, when Co^{III}corroles were functionalized on the gold electrodes, the additional enhancement of electrochemically catalytic behaviors was also observed.[32-33] In the field of photodynamic therapy, ruthenium corroles have become a precise "molecular surgical knife" for anti-cancer treatment due to the singlet oxygen yield (Φ_Δ>0.8) excited by near-infrared light.[34]

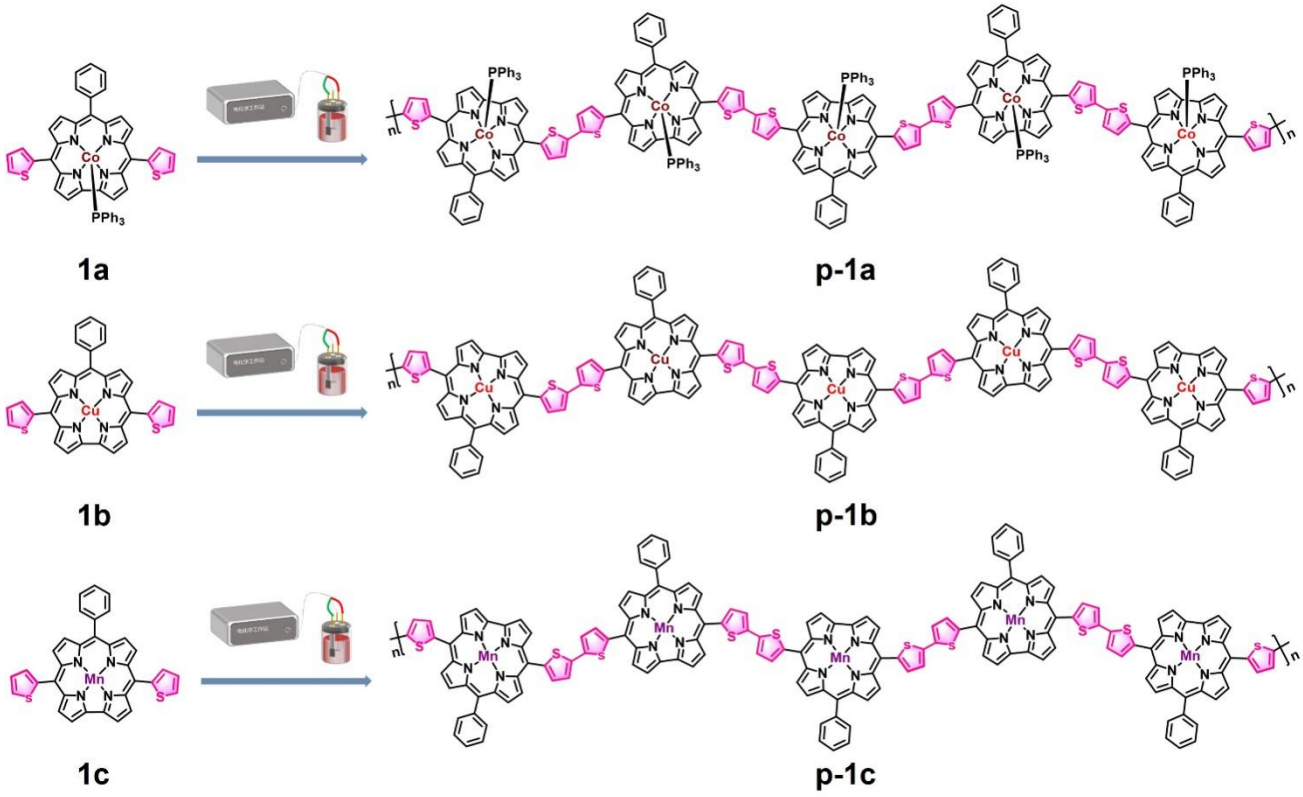

Scheme 1. The general electropolymerzation methods of metallocorroles based polymers **p-1a-c**.

Till now as our best knowledge, the electropolymerized linear shape Co^{III}corrole polymers have exhibited the more satisfied electrocatalytic hydrogen evolution behaviors, and their electrocatalytic behaviors could be accelerated through co-polymerization with thiophene derivatives or changing the electronic structure of metallocorrole monomers.[35-36] Based on the all advantages of above mentioned metallocorroles and polymers, we herein designed three metallocorroles with different metal-centers including cobalt, manganese and copper, and their electrochemically catalyzed oxygen reduction behaviors were also investigated.

Experimental

General

The preparation of metallocorrole monomers including $Co^{III}PPh_3$corrole **1a**, Cu^{III}corrole **1b** and Mn^{III}corrole **1c** was carried out according the literature reported procedures.[37] The metallocorrole based conductive polymers were prepared through the electrochemical polymerization method, and the three-electrode cyclic voltammetry method was used (working electrode: carbon paper electrode (platinum clip), auxiliary electrode: platinum wire, and reference electrode: Ag/AgCl electrode). The carbon paper electrode was selected the hydrophilic type with 1 cm^2 surface area (the actual area is about 0.8 cm^2). Before use, the carbon paper electrode was cleaned with the mixed organic solvent (ethanol:acetone = 1:1; v/v) through ultrasonication for 10 min to remove oil and impurities on the surface of the carbon paper. The electrochemical polymerization was applied in the mixed solution of CH_2Cl_2/CH_3CN (3:2, v/v) solution containing 0.1 M metallocorrole **1a-c** as the monomers and 0.1 M tetraethylammonium tetrafluoroborate (TEAT) as the supporting electrolytes. In addition, the electrochemical polymerization was performed within the potential range of E = –1.8 V to 1.5 V (*E vs.* Ag/AgCl), and the modulation the metallocorrole polymers including electropolymerized Co^{III}corrole **p-1a**, Cu^{III}corrole **p-1b** and Mn^{III}corrole **p-1c** were achieved by changing the different scan rates and polymerization cycles (Scheme 1). Thus, the most satisfied polymerization parameters for subsequent electrocatalytic tests could be obtained.

Preparation of Electrodes

After preparing the metallocorrole-based conductive polymers through electropolymerization, the conductive polymers, which were separated in the solution, were used. In order to well construct the electrodes, we firstly prepared a mixed solution contain 2 mg multi-walled carbon nanotubes (MWCNT), 1 mL isopropanol and 40 μL Nafion perfluorinated resin, and dispersed by ultrasound for 30 min. For the electrocatalytic hydrogen evolution (HER) test, 2.5 μL of above prepared MWCNT solution was dropped onto the surface of a glassy carbon (GC) electrode (Φ = 0.25 cm). After the surface of GC electrode has been well dried, 4.0 μL of metallocorrole **p-1a-c** based polymer solutions were dropped to provide a uniformly dense polymer film covering the electrode surface. For the electrocatalytic ORR test, 4.0 μL of above prepared MWCNT, 6.0 μL of metallocorrole **p-1a-c** based polymer solution, and the central-GC (Φ = 0.4 cm) coated rotating ring disk electrode were used instead.

Electrochemical Catalysis

The metallocorrole based conductive polymer modified GC electrodes were used as the working electrode, platinum wire was used as the electrode, and the calomel electrode (for oxidation/reduction reaction, ORR) and/or Ag/AgCl electrode (for HER) were used as the reference electrodes. In addition, the electrochemically catalyzed oxygen reductions were measured in 0.1 M KOH with the test potential range of electrocatalyzed oxygen reductions are E = –0.9~0.1 (*E vs.* Hg/Hg_2Cl_2) with saturated nitrogen and saturated oxygen at a scanning speed of 100 mV/s, respectively. Upon changing the rotational speed (400~1600 rpm) in a saturated oxygen solution, the Rotating ring-disk electrode (RRDE) polarization curves were with a scanning speed of 10 mV/s. Also, the RRDE polarization curves were obtained in saturated nitrogen and saturated oxygen solutions at 1600 rpm. Meanwhile, the electrochemical impedance spectroscopy (EIS) measurements were tested in a mixed solution of potassium ferrocyanide (KCl 0.1 mol/L, $K_4Fe(CN)_6{\cdot}3H_2O$ 5 mmol/L, $K_3Fe(CN)_6$ 5 mmol/L) at E = –1.2 V; Change the scan rate to 5, 10, 15, 20, 25, and 30 mV/s in 0.1 M KOH to test the CV curve and calculate the double-layer capacitance. Finally, in a 0.1 M KOH solution dissolved in saturated nitrogen at a speed of 1600 rpm.

Results and Discussion

Characterizations of metallocorrole monomers

Metallocorroles generally have two major absorption bands at around λ = 400 nm (Soret-band) and 600 nm (Q-band). Upon introducing different *meso*- and/or β-substituents, coordinating metal-centers, and axial ligands, the absorption properties will be changed. As shown in Figure 1, in CH_2Cl_2, these metallocorroles have Soret and Q-band absorptions at λ = 387 and λ = 562 nm for Co^{III}corrole **1a**, λ = 420, 543 and λ = 644 nm for Cu^{III}corrole **1b** and λ = 538 and 613 nm for Mn^{III}corrole **1c**. Comparing with regular metallotriphenylcorroles, **1a-c** have red-shifted absorption bands by introducing electron-donating thiophene-units and *meso*-5,15-positions. In addition, these three metallocorroles have similar FT-IR spectra, but the major difference were concentrated at 1600–900 cm^{-1}. In Figure 1 (right), the peaks appearing at 3121–2835 cm^{-1} were assigned by the stretching vibration of C-H on the pyrrole benzene ring, the peaks at 1750–1452 cm^{-1} are the skeletal vibration of the pyrrole and benzene ring, and the peak at 1150–960 cm^{-1} indicates the presence of M-N formed by transition metals and N inside the corrole rings.

Electropolymerization

As shown in Figure 2, by comparing the cyclic voltammetry curves of metallocorroles **1a-c** and **p-1a-c** before and after 100 cycles of electropolymerization at a scanning rate of 100 mV/s, it has been found that the CV curves tend to flatten out with the progress of polymerization, and no obvious oxidation-reduction peaks are formed after polymerization. This is due to the decrease in the solubility of the conductive polymer during the electrochemical polymerization progresses, and the current density gradually decreases. Based on the above results, the plausible mechanism of thiophene-substituted metallocorroles is similar to that of thiophene, so called α-H oxidative coupling, expect the electrochemical process was applied. During the electropolymerization, the hydrogen atom at the α-position of thiophene ring to detach and form a free radical cation two thiophene-substituted metallocorrole free radicals couple to form a dimer, or continuous oxidative coupling occurs between free radicals to form a polymer. The attack of hydrogen radical cation on other sites of thiophene promotes its irreversible oxidation process.

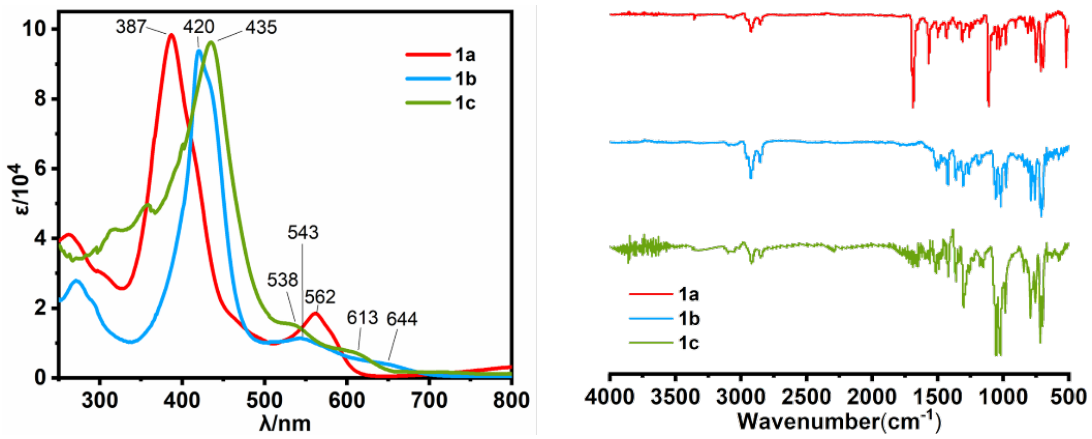

Figure 1. UV-vis (in CH_2Cl_2, left) and FT-IR (right) spectra of metallocorroles **1a-c**.

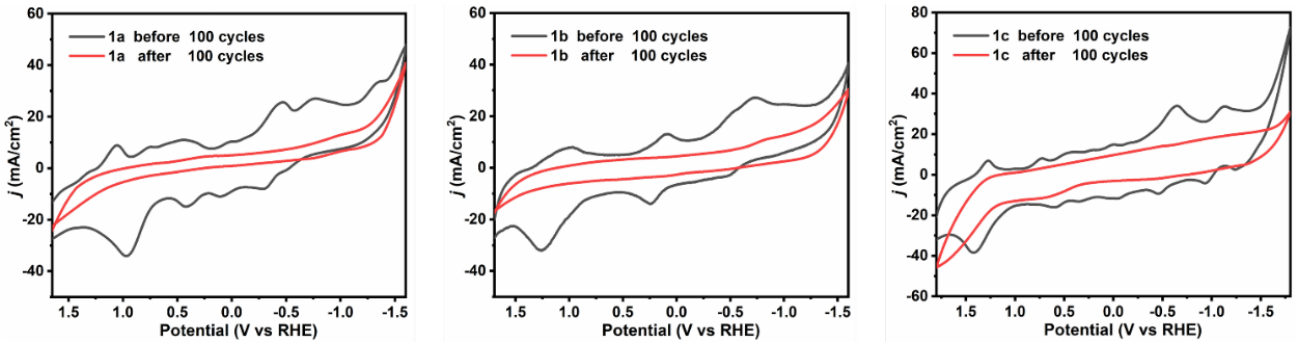

Figure 2. Cyclic voltammetry curves of metallocorroles **1a-c** and metallocorrole based polymers **p-1a-c**.

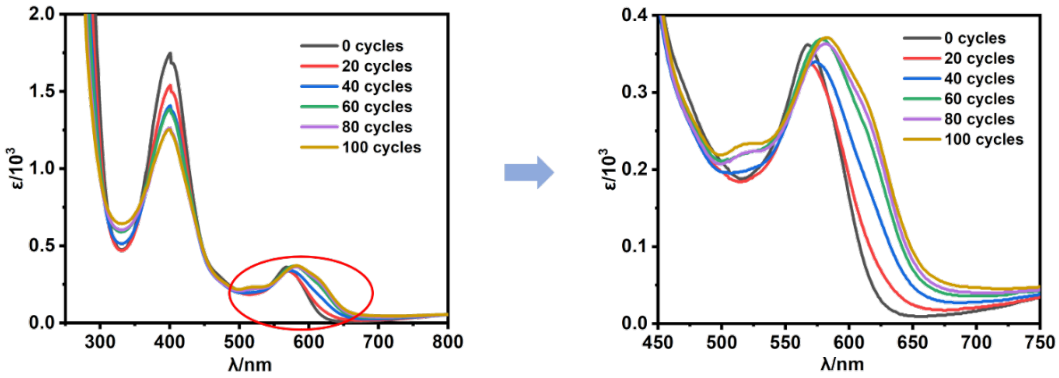

Figure 3. UV-vis spectra of Co^{III}corrole based polymer **p-1a** with different polymerization cycles in CH_2Cl_2 at 298K.

In order to confirm the structure of thiophene-based polymers, we tested high-resolution electrospray ionization mass spectrometry (ESI-MS) of electropolymerized Co^{III}corrole **p-1b**. When we analyze the mass to charge ratio (*m/z*) of ions between 400 and 3000, the observed peaks can indicate the Co^{III}corrole based polymer **p-1a** was formed with different polymerization degrees. Similarly, we also confirmed the mass spectra of Cu^{III}corrole based polymer (**p-1b**) with different polymerization degrees. On the other hand, we have prepared Co^{III}corrole based polymer **p-1a** with 20, 40, 60, 80, and 100 scanning cycles to compare the relationship between different polymerization degrees and spectroscopic properties. As shown in Figure 3, the UV-vis of Co^{III}corrole based polymer **p-1a** with different polymerization degrees exhibited the characteristic Soret and Q bands. However, the shape of absorption bands was gradually expanded with the number of polymerization cycles, especially the Q-bands have been clearly red-shifted. This phenomenon could be explained as the expansion of Co^{III}corrole π-conjugation system to form a smaller HOMO-LUMO gap and red-shifted main absorption bands.

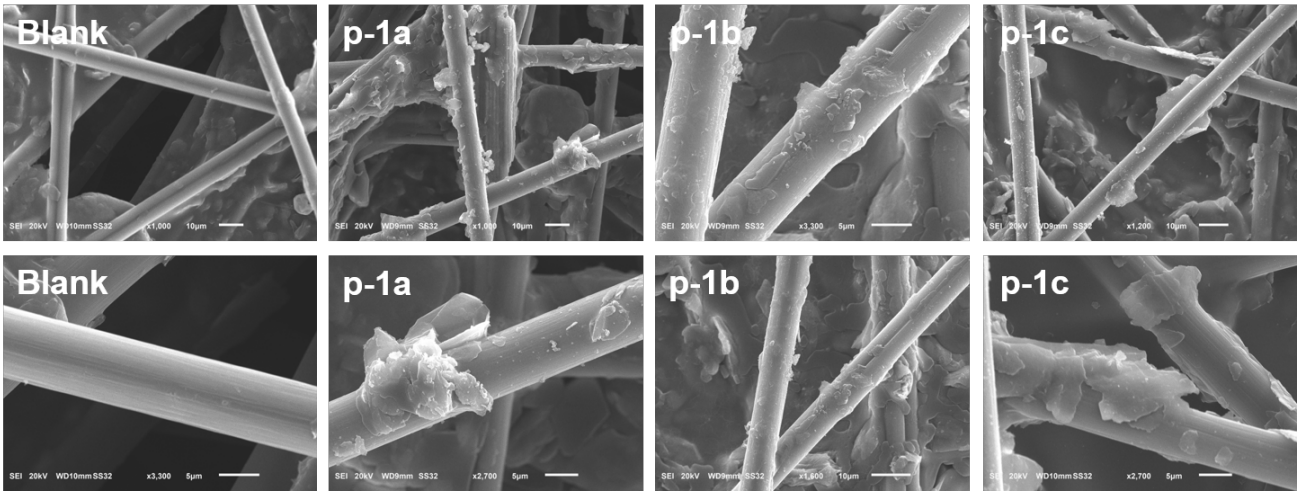

Figure 4. Scanning electron microscopy images of bare carbon paper and metallocorrole based polymers **p-1a-c**.

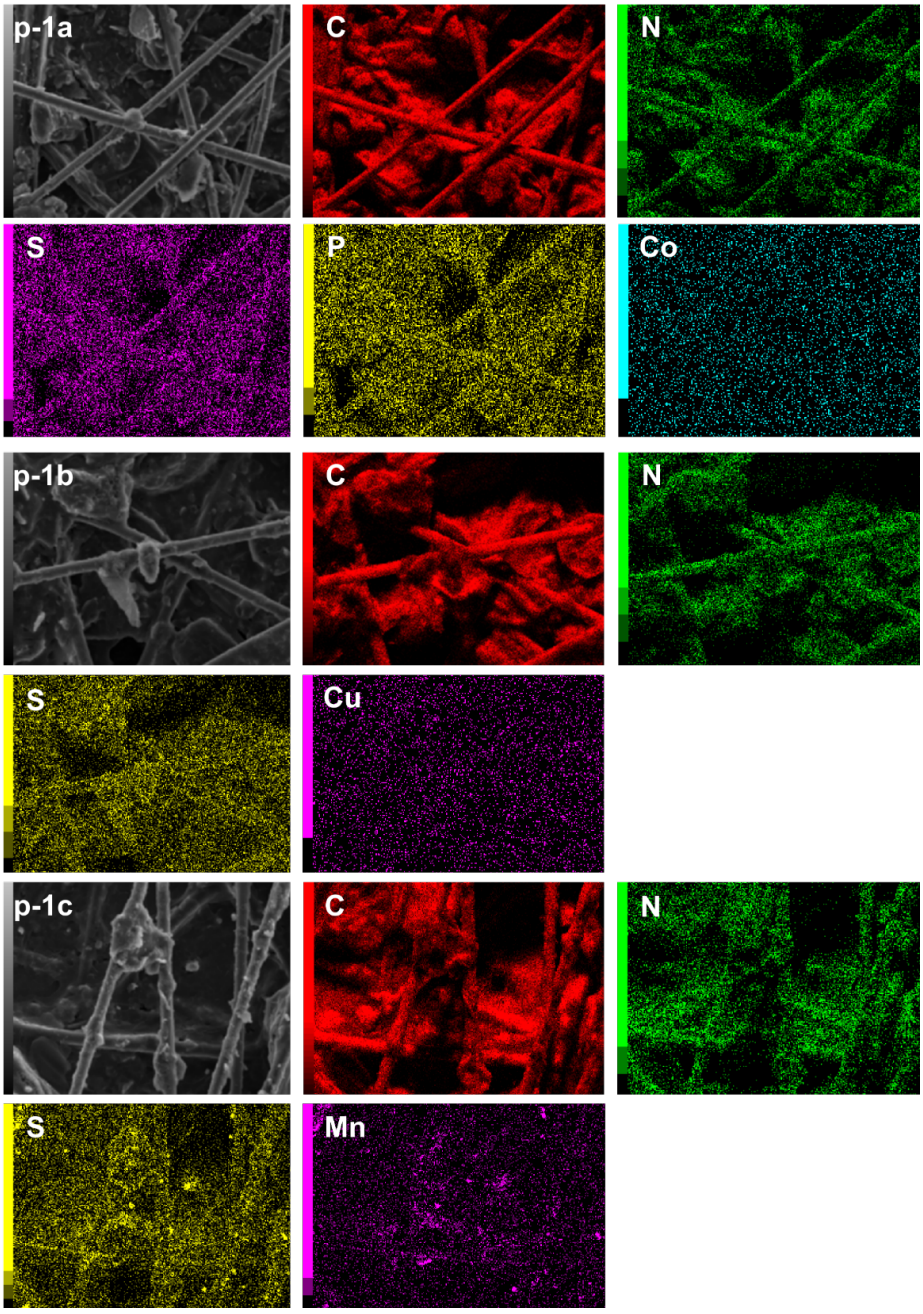

Figure 5. EDS mapping analysis of metallocorrole based polymers **p-1a-c.**

In order to further confirm the morphological characteristics of metallocorrole based polymers **p-1a-c** by comparing with their related monomers, the scanning electron microscopy (SEM) was applied and the carbon paper was used as the supporters. As shown in Figure 4, the bare carbon paper has a pure smooth carbon fiber structure, while the metallocorroles **1a-c** all have the amorphous material structures on the carbon paper surface. On the other hand, metallocorrole based polymers **p-1a-c** exhibited the thin layered sheet structure with 2–5 μm diameters. In addition to confirm the formation of different elements, the EDS analysis (energy dispersive spectrometer) was used to investigate the C, N, S, P elemental analysis of metallocorrole based polymers **p-1a-c**. Figure 5 shows the distribution of elements (C, N, S, P, and M) in the polymerized conductive polymers **p-1a**, **p-1b**, and **p-1c**. Based on the distribution of bright spots and density in the figures, the unique elements of the compounds are displayed, which highly matches the distribution in the SEM image. This once again indirectly verifies the successful synthesis of conductive polymers.

Electrochemical Catalysis

In addition, the electrochemical impedance spectroscopy of metallocorroles **1a-c** and its electropolymerized **p-1a-c** to were tested to confirm the electronic conductivity of their functionalized GC electrodes. This is because the relationship between polymer conductivity and catalytic activity is explored by studying the effect of polymer films on electron transfer on electrode surfaces. In EIS testing, we used an equivalent circuit model to fit the R (CR) model. The diameter of the semicircle in the figure corresponds to the charge transfer resistance (Rct), and the smaller diameter indicates the faster surface charge transfer. In Figure 6, the trends of semi-circular diameter were ordered as **1a** (861Ω) < **1c** (1183Ω) < **1b** (1378 Ω) which corresponding to the smaller resistance faster electron transfer process. Upon electropolymerization, the trends of semi-circular diameter of three polymers are similar with the related monomers in the order of **p-1a** (861Ω) < **p-1c** (1183Ω) < **p-1b** (1378 Ω), but are all smaller than the related monomers. To evaluate the catalytic activity of conductive polymers, we further analyzed the electrochemical catalytic active area, namely the double layer capacitance (C_{dl}). In 0.1 M KOH, we tested the CV curves and calculated the double-layer capacitance using 5, 10, 15, 20, 25, and 30 mV/s. As shown in Figure 7, the double-layer capacitance of **p-1a** (3.15 mF/cm^2) is greater than that of **p-1b** (2.18 mF/cm^2) and **p-1c** (2.88 mF/cm^2), indicating that the conductive polymer of **p-1a** has a larger electrochemical active surface area, followed by **p-1c** and finally **p-1b**. Compared to monomers, conductive polymers greatly enhance their electrochemical active surface area, which is consistent with the trend of EIS testing.

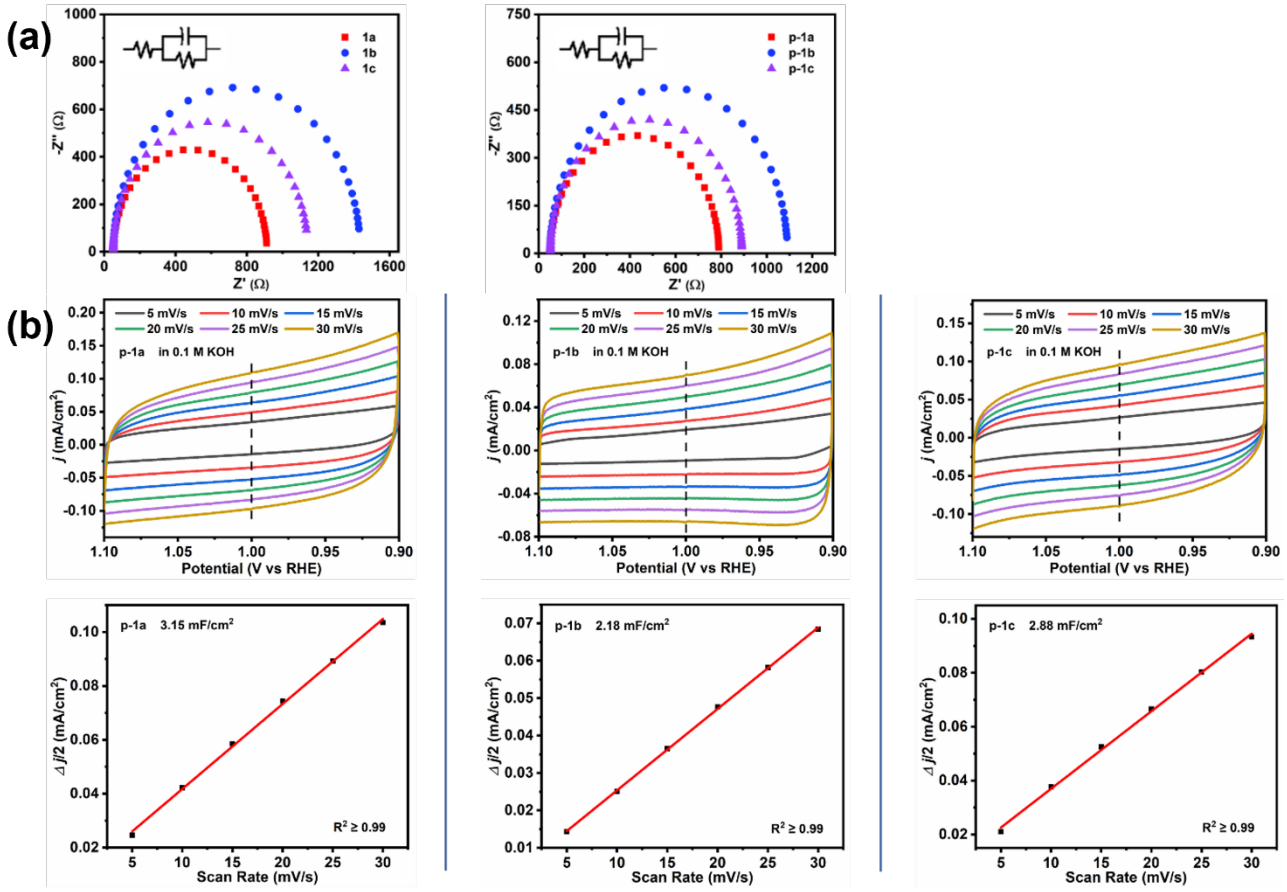

Figure 6. (a) EIS measurements and (b) the double-layer capacitances of metallocorroles and their related polymers **p-1a-c**.

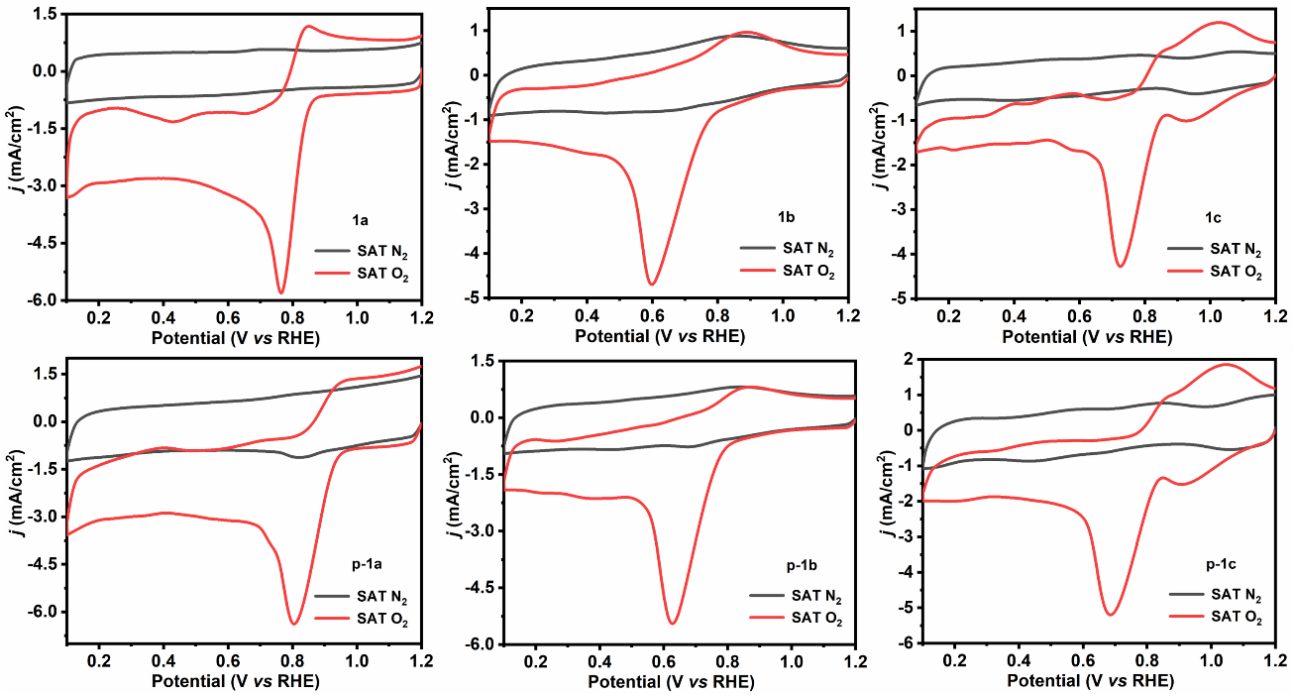

Figure 7. Cyclic voltammetry curves of metallocorrole monomers and their conductive polymers in 0.1M KOH saturated by N_2 and O_2.

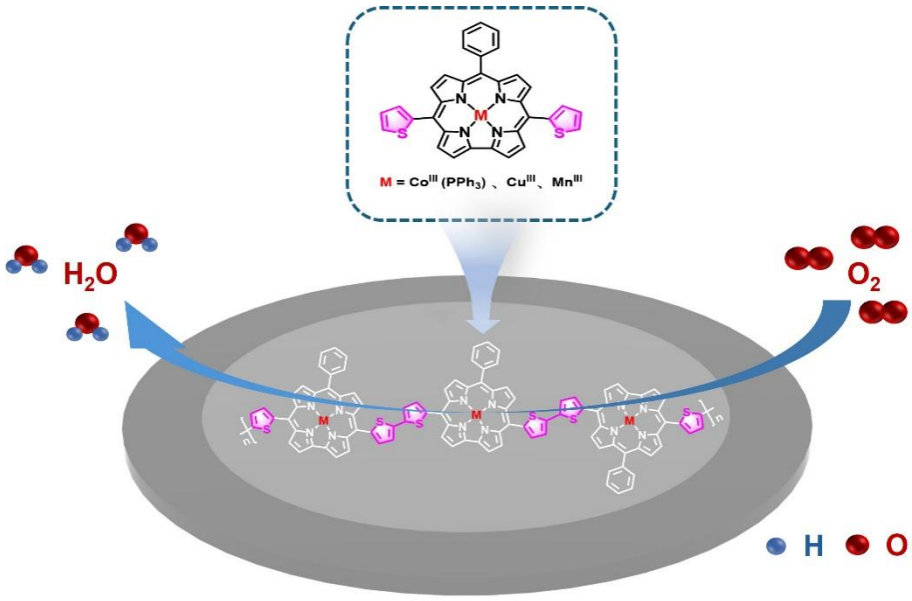

Scheme 2. The plausible mechanism of enhanced electrocatalytic ORR of **p-1a-c**.

To verify the electrochemical catalytic oxygen reduction activity of three metallocorroles and their polymers, we used a rotating disk electrode to measure the CV curves (*E* = 0.1–1.2V; *E vs.* RHE) in 0.1 M KOH solutions containing saturated nitrogen and oxygen, respectively. As shown in Figure 7, both metallocorroles **1a-c** and their related polymers **p-1a-c** (40 cycles electropolymerization) all exhibited the oxygen reduction catalytic activity, and the polymers **p-1a-c** show the positive-shift of potential values, which demonstrating that the metallocorrole based polymers with expanded conjugation system have the better electro-catalytic ORR activity (Scheme 2).

In order to investigate the effect of electrochemical polymerization degree on catalytic performance, we achieved regulation by controlling the number of polymerization cycles. As shown in Figure 8 and Table 1, we prepared metallocorrole based polymers **p-1a-c** with of 20, 40, 60, 80, and 100 polymerization cycles, and their RDE polarization curves were measured at a 10 mV/s scan rate with the 600 rpm rotation speed. When the 40 cycles of electropolymerization were applied, all three polymers **p-1a-c** exhibited the positive-shift of onset and half-wave potential values, as well as the higher current densities. These results indicate that the 40 cycles are suitable conditions of electrochemical polymerization which have the better electrocatalytic ORR performance. Furthermore, the RDE polarization curves of three polymers **p-1a-c** were also tested after 40 cycles of polymerization at of 400, 625,

900, 1225, and 1600 rpm rotating disk electrode speeds. As shown in Figure 8b, with the continuous increase of rotational speed, the diffusion current uniformly increases, indicating that the oxygen reduction reaction on the electrode surface is diffusion controlled. On the other hand, the electron transfer numbers (n) of the ORR process were also calculated by using the K-L equation (Figure 8c, Table 1), and the electron transfer numbers of polymers **p-1a-c** were n = 3.67, 3.43, and 3.63, respectively. Compared to the oxygen reduction of electron transfer numbers metallocorroles **1a** (2.87), **1b** (2.75), and **1c** (2.84), the electropolymerized **p-1a-c** significantly improved their ORR performance and tended to be converted to water through four electron oxygen reduction.

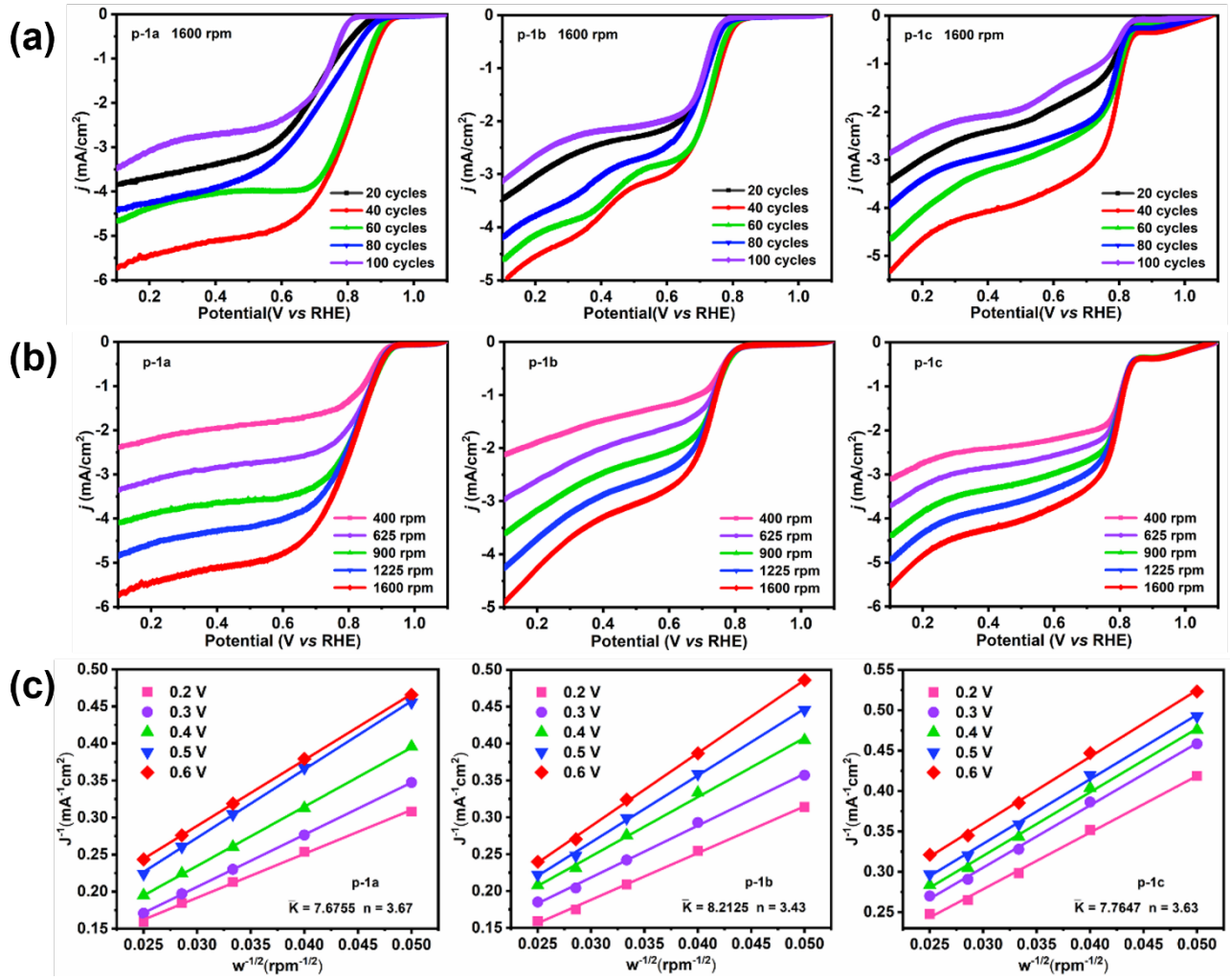

Figure 8. RDE polarization curves with different number of polymerization cycles (a) different rotating speeds (b); K-L curves of conductive polymers **p-1a-c** (c).

Table 1. The summary of E_{onset}, $E_{1/2}$ and n data of metallocorrole **1a-c** and their related polymers **p-1a-c**.

No.	Onset-potentials (V)	Half-wave Potentials (V)	n (RDE)
1a	0.88	0.78	2.87
1b	0.74	0.68	2.75
1c	0.85	0.76	2.84
p-1a	0.91	0.80	3.67
p-1b	0.77	0.71	3.43
p-1c	0.87	0.77	3.63

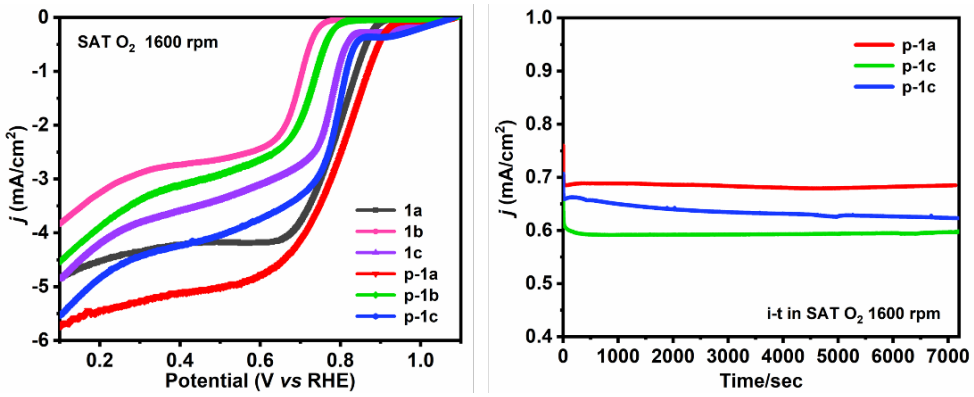

Figure 9. RDE polarization curves (left) of metallocorrole monomers and their conductive polymers and *i*-t curves (right) of conductive polymers.

More importantly, the RDE polarization curves of metallocorroles **1a-c** and their related polymers **p-1a-c** were compared at 1600 rpm rotating speed. As shown in Figure 9 and Table 1, it can be seen that all three metallocorrole based polymers **p-1a-c** have the positive-shift of onset and half-wave potential values compared to their monomers **1a-c**. Among them, the Co^{III}corrole based polymer **p-1a** has the best electrocatalytic performance with onset and half-wave potential values at E = 0.91 and 0.80 V, respectively. The trends were followed by Mn^{III}corrole based polymer **p-1c** (0.85 and 0.76V) and Cu^{III}corrole based polymer **p-1b** (0.74 and 0.68V). This result indicates that the metal centers have the significant influence impact on the electrochemical catalytic performance. At the same time, the *i*-t curves of metallocorrole based polymers **p-1a-c** were also tested by chronoamperometry at 1600 rpm in 0.1 M KOH containing saturated oxygen for 7200s (Figure 9b). Within 7200 seconds, all three polymers **p-1a-c** exhibited stable peak currents (*j* values), which demonstrating good catalytic stability for all three polymers. The current intensity was **p-1a** > **p-1c** > **p-1b**, consistent with the trends we obtained in other electrochemical tests. Meanwhile, we have compared the electrochemically catalyzed oxygen reduction behaviors of a series of metallcorrole based catalysts (Table S1, details see ESI), the metallocorrole based polymers **p-1a-c** are the most satisfied catalyst for electrocatalyzed oxygen reduction to water through selective four electrons ($4e^-$) oxygen reductions.

Conclusion

In summary, a series of three M^{III}corrole monomers (M = Co, Cu, Mn) were prepared, and the related polymers were prepared through facile and environmentally friendly electropolymerizations. In addition, these polymers were characterized by mass, SEM and EDS mapping analysis. Upon functionalized on the electrodes, these metallocorrole based polymers with expanded material structures exhibited the smaller resistance and the higher double layer capacitance. In addition, these polymers exhibited the enhanced and tunable electrochemically catalyzed oxygen reduction reactions, and the electron transfer numbers (n) of the ORR process of three polymers **p-1a-c** were n = 3.67, 3.43, and 3.63 which tended to be converted to water through selective four electrons (4e-) oxygen reductions, especially the Co^{III}corrole based polymer **p-1a** has the most satisfied performance. Considering highly conjugated conductive polymers have the wide range of applications in several high-tech fields, the current investigation may provide useful information for future design, characterization and application of novel functional conjugated materials.

Acknowledgements. This work was supported financially by the NaturalScience Foundation of China (21701058), Jiangsu University (17JDG035), the Innovation Project of Jiangsu Province 2023 and the Educational Science Planning Project of Jiangsu Province (B/2022/01/129).

Conflicts of interest. The authors can declare that there are no known competing personal relationships or financial interests that could be perceived as having influenced the research reported in this study.

Author contributions. Yu Chen, Minyu Jiang, Shibin Zhu and Yunlong Pan focused on the material preparation and electrochemical characterizations; Jing Xu and Xu Liang focused on the manuscript preparation and the whole work was well discussed by all authors.

References

1. Chiang C.K., Fincher C.R.,Jr., Park Y.W., Heeger A.J., Shirakawa H., Louis E.J., Gau, Alan G. MacDiarmid. *Phys. Rev. Lett.* **1977**, *39*(17), 1098–1101.
2. Yamabe T., Tanaka K, Terama-e H., Fukui K., Imamura S., Shirakawa H., Ikeda S. *J. Phys. C: Solid State Phys.* **1979**, *12*(7), L257.
3. Bustamante C.M., Scherlis D.A. *PCCP* **2021**, *23*, 26974–26980.
4. Gmucová K. *Curr. Opin. Electrochem.* **2022**, 36, 101117.
5. Ke Sh., Chen T., Nie X., Ai X., Huang T., Zhang H., Li L., Xu W., Liu Ch., Zhu W., Wei P., He D., Zhao W., Zhang Q. *J. Mater. Chem. A* **2024**, *12*, 9787–9796.
6. Schauer F., Nádaždy V., Gmucová K., Váry T. *J. Appl. Phys.* **2018**, *124*, 165702.
7. Wang X., Hu X., Zhai X., Huang X., Li Zh., Zou X., Shi J. *J. Food Meas. Charact.* **2024**, *18*, 5813–5825.

8. Li Zh., Zhou X., Shi J., Zou X., Huang X., Haroon E.T. *Food Chem.* **2019**, *276*, 291–297.
9. Chen A.H., Liang H.X., Chen T.M., *et al. Sci. Rep.* **2017**, *7*, 44562.
10. Wang H., Li Z., Zuo M., Zeng X., Tang X., Sun Y., Lin L. *Carbohydr. Polym.* **2022**, *280*, 119018.
11. Masood M., Hussain S., Sohail M., Rehman A., Uzzaman M.A., Alnaser I.A., Karim M.R., Wahab M.A. *Chemistry Select* **2024**, *9*, e202302876.
12. Namsheer K., Chandra Sekhar Rout *RSC Adv.* **2021**, *11*, 5659–5697.
13. Guven N., Yucel B., Sultanova H., Camurlu P. *Dyes Pigm.* **2022**, *205*, 110526.
14. Wang J., Hui N. *Sens. Actuators, B* **2019**, *281*, 478–485.
15. Liustrovaite V., Ratautaite V., Ramanaviciene A., Ramanavicius A. *Biosens. Bioelectron.* **2024**, *272*, 117092.
16. Joo Y., Agarkar V., Sung S.H., Savoie B.M., Boudouris B.W. *Science* **2018**, *359*, 1391–1395.
17. Zhao Y., Zhang L., Lv M., Jiao Ch., Cheng P., Fu Y., Li J., Liu Q., He D. *ACS Appl. Mater. Interfaces* **2021**, *13*, 31171–31179.
18. An M., Bai Q., Jeong S.Y. , Ding J., Zhao Ch., Liu B., Liang Q., Wang Y., Zhang G., Woo H.Y., Qiu X., Li Niu, Guo X., Sun H. *Adv. Eng. Mater.* **2023**, *13*, 2301110.
19. Eftekhari A., Li L., Yang Y. *J. Power Sources* **2017**, *347*, 86–107.
20. Quijada C. *Materials* **2020**, *13*, 2344.
21. Ooi Sh., Tanaka T., Osuka A. *Inorg. Chem*. **2016**, *55*, 8920–8927.
22. Gross Z. *J. Biol. Inorg. Chem.* **2001**, *6*, 733–738.
23. Lei H., Li X., Meng J., Zheng H., Zhang W., Cao R. *ACS Catal.* **2019**, *9*, 4320–4344.
24. Tesakova M.V., Vikol L.K., Kuzmin S.M., Parfenyuk V.I. *ChemChemTech* **2022**, *65*(5), 58–67, doi: 10.6060/ivkkt.20226505.6554.
25. Zou B., Liu F., Yan Y. Food Chem. **2022**, *388*, 132898.
26. Song F., Wang B., Shi Zh-J. *Acc. Chem. Res.* **2023**, *56*, 2867–2886.
27. Zhang Z., Dai W. *Chem Catal*. **2021**, *1*, 1352–1353.
28. Speiser Sh., Schael F. *J. Mol. Liq.* **2000**, *86*(1–3), 25–35.
29. Boateng I.D., Yang X.-M. *Ind. Crops Prod.* **2021**, *162*, 113287.
30. Lopes J.M.S., Machado A.E.H., Batista A.A., Iglesias B.A., Araujo P.T., Barbosa Neto N.M. *J. Photochem. Photobiol., A* **2023**, *438*, 114568.
31. Rana A., Lee Y.-M., Li X., Cao R., Fukuzumi Sh., Nam W. *ACS Catal.* **2021**, *11*, 3073–3083.
32. Kumar A., Fite Sh., Raslin A., Kumar S., Mizrahi A., Mahammed A., Gross Z. *ACS Catal.* **2023**, *13*, 13344–13353.
33. Nardis S., Mandoj F., Stefanelli M., Paolesse R. *Coord. Chem. Rev.* **2019**, *388*, 360–405.
34. Zhou Da, Zuo Junbo, Zeng Chenghao, Li Zhang, Xuejin Gao, Guoli Li, Xinying Wang *Nutrition* **2024**, *125*, 112472.
35. Jiang M., Li M., Zhang X., Zhu W., Liang X. *J. Electroanalyt. Chem.* **2024**, *965*, 118344.
36. Ma G., Shi Q., Hou X., Peng Y., Liu Q. *Front. Sustain. Food Syst.* **2024**, *8*, 1448421.
37. Sun R., Liu M., Wang P.,Qin Y., Schnedermann Ch., Maher A.G., Zheng Sh.-L., Liu S., Chen B., Zhang Sh., Dogutan D.K., Lindsey J.S, Nocera D.G. *Inorg. Chem.* **2022**, *61*, 12308–12317.

Received 21.04.2025
Accepted 30.05.2025